19th Brazilian Congress of Thermal Sciences and Engineering
November 6th–10th, 2022, Bento Gonçalves - RS - Brazil

ENC-2022-0074
DATA-BASED MODAL DECOMPOSITION OF OSCILLATORY METHANE JET DIFFUSION FLAMES

Fernanda Spilotros Costa Cordeiro
Leonardo Santos de Brito Alves
Luiz Carlos da Silva Nunes
Juan Carlos Assis da Silva
Departamento de Engenharia Mecânica, Universidade Federal Fluminense, Rua Passo da Pátria 156, Bloco E, Sala 211, Niterói, RJ 24210-240, Brazil.
fernandacordeiro@id.uff.br, lsbalves@id.uff.br, luizcsn@id.uff.br, jcasilva@id.uff.br

Abstract. *Modal decomposition is widely used to characterize disturbance behavior in unstable dynamical systems. Most of these techniques are based on the singular value decomposition (SVD), since it provides a systematic way to generate an accurate low-dimensional approximation of a high-dimensional data set. Different modal decomposition's are compared in the present paper, as they are applied to identify dominant oscillatory disturbances in methane jet diffusion flames. The techniques evaluated here are proper orthogonal decomposition (POD) and dynamic modal decomposition (DMD).*

Keywords: *modal decomposition, singular value decomposition, low-dimensional approximation, proper orthogonal decomposition, dynamic modal decomposition*

1. INTRODUCTION

The study of turbulent flows belongs to a challenging area of fluid mechanics. Numerous techniques have been developed to describe turbulent flow, but for the problems of the modern era, empirical models or derivations based on first-principles are not considered sufficient. It is necessary, and intriguing, to understand what happens beyond the transition from laminar to turbulent flow, and with that model and predict a system that is considered more complex.

Dynamical systems are typically nonlinear, multi-scale in space and time, and high dimensional. With these characteristics, it has become common in flow analysis to look for and extract dominant patterns, which must be modeled for prediction, estimation, and control of the system. Identifying the dominant patterns, also known as modes, is the first step in flow analysis, and usually begins with modal decomposition of data from an experimental or numerical data set.

Modal decomposition is progressively being applied to a variety of dynamical systems and revolutionizing the way they are studied. They are a great tool to automatically identify and separate different phenomena in a flow, separating it into its modes. With this, it is possible to reconstruct the original flow using only the dominant modes with main flow characteristics, and thus filter out measurement noise or outliers. In view of this, modal decomposition can be applied to reduce data from an experiment by storing the dominant modes with higher energy content and then reconstructing the original flow from the stored data. Modal decomposition techniques are part of data science, which combines various fields of statistics, scientific methods, artificial intelligence, and data analysis. Consequently, data science is being widely employed in the field of fluid dynamics with the goal of developing new tools, which correctly identify the dynamics of the problem and generalize its behavior.

The basis for many modal decomposition techniques is the singular value decomposition, which was discovered about 100 years ago by Eugenio Beltrami (1835-1899) and Camille Jordan (1838-1921). Widely known only as SVD, this technique provides a numerically stable matrix decomposition, obtaining a low-rank approximation for matrices, in order to find the solution of systems of equations. In this paper, oscillatory methane jet diffusion flames will be analyzed using two types of modal analysis, which are POD (Lumley *et al.,* 1993), i.e. **P**roper **O**rthogonal **D**ecomposition, and DMD (Brunton *et al.,* 2016), i.e. **D**ynamic **M**ode **D**ecomposition. The methane jet experiment was performed inside an acoustic chamber, which creates disturbances to the jet flame at certain frequencies. The parameters selected during the execution of the experiment were Reynolds number equal to 40, acoustic forcing frequency equal to 332 Hz and maximum pressure of 100 Pa. Therefore, each modal decomposition technique will be defined and will be used to model the dynamic system of jet flames, and will later be compared to examine their results.

2. IMAGE PROCESSING

Digital image processing refers to processing images by a digital computer. For instance, from image processing algorithms experimental image data can be enhanced. After processing, in addition to the enhancement of the images, it is possible to extract some useful information for further analysis.

Images extracted from experiments often contain some random noise, which makes further analysis difficult. In many applications, it is necessary to distinguish between what is a signal from the experiment and noise, to finally study the behavior of the chosen phenomenon. Basically, this type of processing encompasses 3 general phases that all kinds of data have to undergo, which are pre-processing, restoring the image and information extraction.

Early methods for image restoration were based on least squares, and had the disadvantage of smoothing edges or creating false oscillations near the edges. In the case of digital images, most commonly used today, the most noticeable features are edges and textures, and therefore there are more efforts to study modified models, with the goal of eliminating noise while preserving edges and small-scale features. Among the new methods, variational models have been extremely successful in a wide variety of image restoration problems, a typical model being the ROF variational model, which was developed by **R**udin, **O**sher, and **F**atemi (Rudin *et al*, 1992). Consider the degradation image modeled as follows:

$$f = u + \eta \tag{1}$$

where f is the observed image from the experiment, u is the original image and η is the noise.

Therefore the ROF image processing is written as follows

$$\min_{u \in BV(\Omega)} (\frac{1}{2}||u - f||^2_{L^2} + \lambda |u|_{BV}) \tag{2}$$

where λ is a parameter that corresponds to noise removal and BV is a Banach space, that is a complete normed space. In view of this, the ROF image processing is categorized as a denoising problem.

In conjunction with the ROF denoise method, another method was chosen for the image processing of the methane jet experiment, which was the Gaussian filter. The Gaussian filter is considered as a noise reducer in images, like the method mentioned earlier, and is also used to blur certain regions of an image. In this type of filter, a symmetric kernel of odd size is implemented, which passes through each pixel of the region of interest in the image, in order to achieve the desired restoring effect.

In the process of using the Gaussian Filter, the size of the kernel that is used to dismember the image is defined as 3x3. The sizes are usually odd numbers, meaning that the overall results can be computed at the center pixel. The values within the kernel are computed by the Gaussian function, which is represented as

$$G(x, y) = \frac{1}{2\pi\sigma^2} e^{\frac{-x^2+y^2}{2\sigma^2}} \tag{3}$$

where σ is a parameter that also corresponds to noise removal. With higher sigma values, the image becomes more blurred at a wider radius.

3. MATHEMATICAL FORMULATION OF MODAL DECOMPOSITION'S

The discussion in the present paper will begin with the presentation of singular value decomposition (SVD), which is the basis for Proper Orthogonal Decomposition (POD) and Dynamic Mode Decomposition (DMD). Let us consider the large data set below $\mathbf{X} \in C^{n \times m}$

$$\mathbf{X} = \begin{bmatrix} | & | & | & | \\ \mathbf{x}_1 & \mathbf{x}_2 & \cdots & \mathbf{x}_m \\ | & | & | & | \end{bmatrix}. \tag{4}$$

Columns $\mathbf{x}_m \in C^{n \times m}$ are experimental measurements acquired through images of the methane jet evolving over time, commonly called snapshots of the experiment. Such columns have been reshaped into column vectors with their elements being the pixels in the images.

The singular value decomposition (SVD) is a unique matrix decomposition, which can be represented as:

$$\mathbf{X} = \mathbf{U\Sigma V^T} \tag{5}$$

where the orthogonal columns belong to the unitary matrices $\mathbf{U} \in C^{n \times n}$ and $\mathbf{V}^T \in C^{m \times m}$. The middle matrix belongs to $R^{n \times m}$, and is represented by the symbol $\mathbf{\Sigma}$. Furthermore, the matrix $\mathbf{\Sigma}$ has real and non-negative entries on the diagonal and zero off the diagonal.

3.1 Proper Orthogonal Decomposition

Within various fields of science, many dynamical systems describe the relationship between space and time of the analyzed phenomenon. Typically, spacio-temporal relationship has complex dynamics and is modeled using partial differential equations. In this case, the proper orthogonal decomposition (POD) is the SVD applied for partial differential equations (PDEs).

This modal decomposition technique, introduced by Lumley (1967), extracts modes with respect to the energy content, providing the most optimal low-ranking decomposition. Increasingly in demand, the reduced order models (ROMs) use the POD modes for projecting PDEs dynamics to low-rank sub-spaces, which enables computational improvements, and allows good simulations of the PDEs. Let us consider the following PDE

$$\mathbf{u}_t = \mathbf{N}(\mathbf{u}, \mathbf{u}_x, \mathbf{u}_{xx}, \cdots, x, t) \tag{6}$$

where the subscripts x and t denote partial differentiation and $\mathbf{N}$ captures the space-time dynamics, that is the nonlinear evolution. To solve the PDE, the variable separation method and basis expansion are used, obtaining the following form

$$u(x,t) = \sum_{n=1}^{\infty} a_n(t)\phi_n(x) \tag{7}$$

where the $\phi_n(x)$ are an orthogonal set of eigenfunctions, called the basis functions. Orthonormality of our basis functions implies that

$$\langle \phi_k \ , \ \phi_j \rangle = \delta_{kj} = \begin{cases} 0 & j \neq k \\ 1 & j = k \end{cases} \tag{8}$$

where the term δ_{kj} is the Dirac function and $\langle \phi_k \ , \ \phi_j \rangle$ is the inner product formulated as follows

$$\langle \phi_k \ , \ \phi_j \rangle = \int_{-L}^{L} \phi_k \phi_j^* \, dx \tag{9}$$

where * means complex conjugation, j is the index for lines and k is the index for columns of the matrix.

Briefly, the optimal POD basis functions are generated from a singular value decomposition (SVD) of the PDE, and it is possible to reshape the system dynamics in the best low-dimensional structure. In addition, the SVD also allows the decomposition of the k^{th} row of $\mathbf{X}$ into

$$\mathbf{X}_k = \sum_{j=1}^{k=N} \sigma_j u_{kj} \phi_j \tag{10}$$

assuming that σ_j are the singular values of $\mathbf{\Sigma}$.

Therefore, the vectors σ_j are the POD modes, which are used to completely reconstruct $\mathbf{X}$. Most of the energy of the PDE dynamical system is concentrated in the first POD modes, which allows few modes to be needed to achieve efficient accuracy during the reconstruction.

3.2 Dynamic Mode Decomposition

Dynamic modal decomposition is a high-dimension reduction technique for data sequences, developed by Peter Schmid (2008). DMD is based on the proper orthogonal decomposition (POD) and singular value decomposition (SVD), but instead of providing modes based entirely on energy content and spatial correlation, ignoring temporal information, DMD provides a modal decomposition where the resultant modes have both spatial and temporal relationship.

DMD is data-driven, and the first step in the decomposition is to collect a number of pairs of snapshots of the state of a system as it evolves in time. Let us consider the snapshots in two matrices

$$\boldsymbol{X} = \begin{bmatrix} | & | & | & | \\ \mathbf{x}(t_1) & \mathbf{x}(t_2) & \cdots & \mathbf{x}(t_m) \\ | & | & | & | \end{bmatrix} \tag{11}$$

$$\boldsymbol{X'} = \begin{bmatrix} | & | & | & | \\ \mathbf{x}(t_2) & \mathbf{x}(t_3) & \cdots & \mathbf{x}(t_{m+1}) \\ | & | & | & | \end{bmatrix} \tag{12}$$

The DMD algorithm searches for the decomposition of the eigenvalues and eigenvectors of the linear operator $\boldsymbol{A}$, which is best suited to relate the two snapshots matrices $\boldsymbol{X}$ and $\boldsymbol{X'}$, as illustrated in the following

$$\boldsymbol{X'} = \boldsymbol{AX} \tag{13}$$

where the matrix $\boldsymbol{A}$ can be defined by $\boldsymbol{A} = \boldsymbol{X}\boldsymbol{X}^{+}$, with $\boldsymbol{X}^{+}$ being the pseudo-inverse of $\boldsymbol{X}$.

Each mode of the DMD is associated with an eigenvalue of type $\boldsymbol{\lambda} = \boldsymbol{a} + \boldsymbol{ib}$, with a specific oscillation frequency $\boldsymbol{b}$ and decay rate $\boldsymbol{a}$. Furthermore, the DMD eigenvalues and modes can be defined as the eigenvalues and eigenvectors of $\boldsymbol{A}$.

Usually, because of the large dimension of $\boldsymbol{A}$, it is not efficient to compute $\boldsymbol{A}$ in a direct way. Instead, SVD is used to optimize the process. Therefore, we rescue equation (2), but use the truncated SVD, considering only the first columns of $\mathbf{U}$, $\mathbf{V}$ and $\boldsymbol{\Sigma}$. This step is done since it reduces the overall dimension

$$\mathbf{X} = \mathbf{U}_{tr}\boldsymbol{\Sigma}_{tr}\mathbf{V}_{tr}^{T} \tag{14}$$

where the subscript $\boldsymbol{tr}$ refers to the truncated SVD, as well as $\mathbf{U}_{tr} \in \boldsymbol{C}^{n\times r}$, $\boldsymbol{\Sigma}_{tr} \in \boldsymbol{C}^{r\times r}$ and $\mathbf{V}_{tr}^{T} \in \boldsymbol{C}^{m\times r}$.

For the truncated SVD, $\boldsymbol{r} \leq \boldsymbol{m}$ for the reason of representing the exact or approximation rank of the data matrix $\mathbf{X}$. Computing the pseudo-inverse of $\mathbf{X}$

$$\mathbf{A} = \mathbf{X}'\mathbf{V}_{tr}\boldsymbol{\Sigma}_{tr}^{-1}\mathbf{U}_{tr}^{T} \tag{15}$$

and applying the POD modes, results in

$$\mathbf{A}_{tr} = \mathbf{U}_{tr}^{T}\mathbf{A}\mathbf{U}_{tr} = \mathbf{U}_{tr}^{T}\mathbf{X}'\mathbf{V}_{tr}\boldsymbol{\Sigma}_{tr}^{-1} \tag{16}$$

Using equation (13), it is possible to find the eigenvalues $\boldsymbol{\mu}$ and eigenvectors $\boldsymbol{v_{tr}}$ of $\mathbf{A}_{tr}$, with $\mathbf{A}_{tr}\boldsymbol{v_{tr}} = \boldsymbol{\mu_j v_{tr}}$. Including, the eigenvalues of the DMD are the nonzero elements of $\boldsymbol{\mu}$. Therefore, the DMD modes are defined as follows

$$\boldsymbol{v} = \boldsymbol{\mu}^{-1}\boldsymbol{X}\boldsymbol{V}_{tr}\boldsymbol{\Sigma}_{tr}^{-1}\boldsymbol{v}_{tr} \tag{17}$$

Commonly, the projected modes of the DMD are computed, where the first $\boldsymbol{r}$ POD modes of the data in X are used

$$\boldsymbol{v} = \mathbf{U}_{tr}\boldsymbol{\mu}^{-1} \tag{18}$$

In conclusion, the growth or decay rates and frequencies of DMD modes are determined by examining the imaginary and real parts of each mode.

4. RESULTS

The first step was to perform image processing on the images from the methane jet experiment. The image processing was done with the following parameters, which are ROF denoise method with $\boldsymbol{\lambda = 14}$ and Gaussian filter with $\boldsymbol{\sigma = 0.2}$. Such parameters change the original image of the experiment and generated a new image with 256x256 pixels and 2000 frames

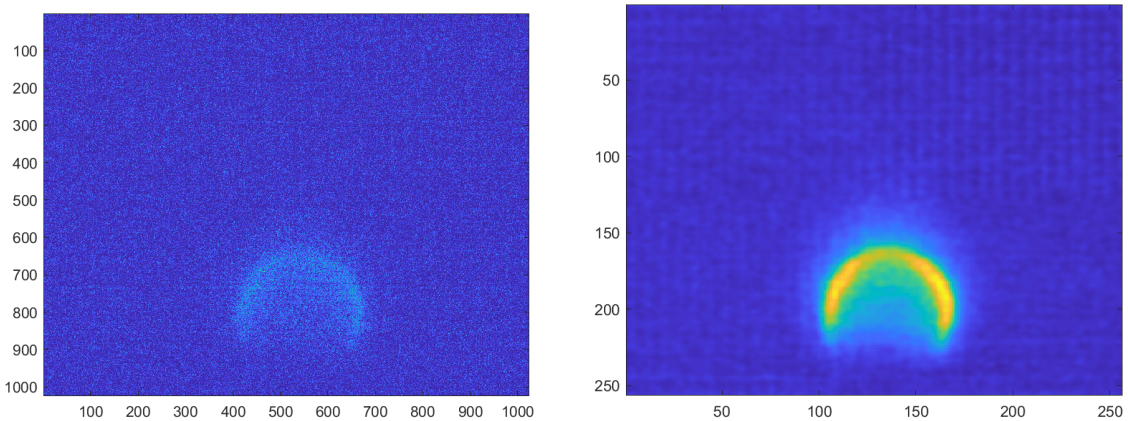

Figure 1. Original experimental image (left) and experimental image after treatment, using ROF denoise with $\boldsymbol{\lambda = 14}$ and Gaussian filter with $\boldsymbol{\sigma = 0.2}$ (right), both with 256x256 pixels and 2000 frames

The next steps, after the image processing, are the modal decomposition analyses. First, the proper orthogonal decomposition (POD) analysis is performed, yielding the following result

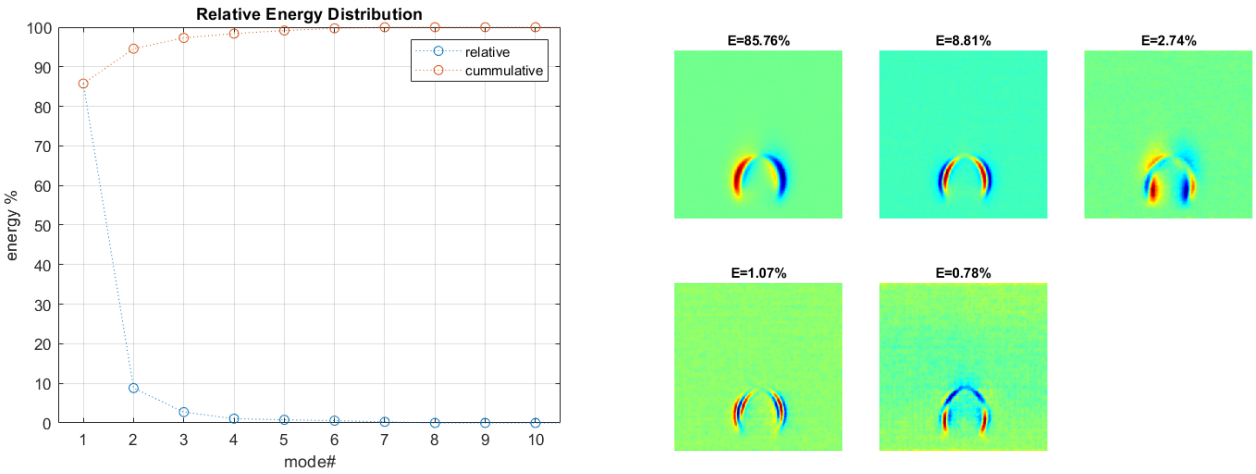

Figure 2. Graphic of relative POD energy distribution (left) and POD modes with their respective energies (right), both graphics acquired after the image processing

The graphic above shows the relationship between relative energy of each POD mode with the accumulated energy. As expected, the first few POD modes accumulate most of the energy of the system, decreasing as the modes progress. However, it is noticeable that after the fifth mode, the noise acquired during the experiment severely interferes with the result of this modal decomposition, making it impossible to visualize later modes.

Furthermore, it can be seen that noise begins to interfere with the fifth mode of the POD by observing the phase portraits below

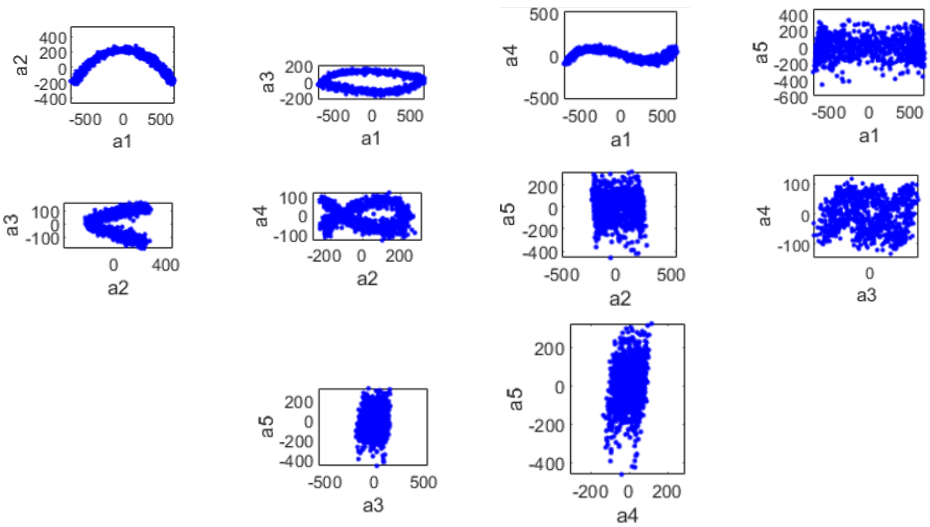

Figure 3. POD phase portraits acquired through image processing with $\boldsymbol{\lambda = 14}$ and $\boldsymbol{\sigma = 0.2}$, which are geometric representations of the trajectories of the methane jet dynamic system in the phase plane. For each set of parameters, a new curve is created, illustrating the behavior of the system.

It can be seen that the graphics containing $\boldsymbol{a5}$, or the fifth mode, and even $\boldsymbol{a4}$, the fourth mode, are uncertain, having no definite relationship with other modes.

Subsequently, the dynamic modal decomposition analysis (DMD) is performed, and the first generated mode corresponds to the mean flame structure

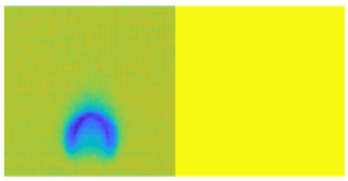

Figure 4. Mean flame structure (right), which represents the first mode of the DMD, having zero oscillation frequency (left)

The rest of the modes, which actually correspond to the dynamics of the system, are represented below

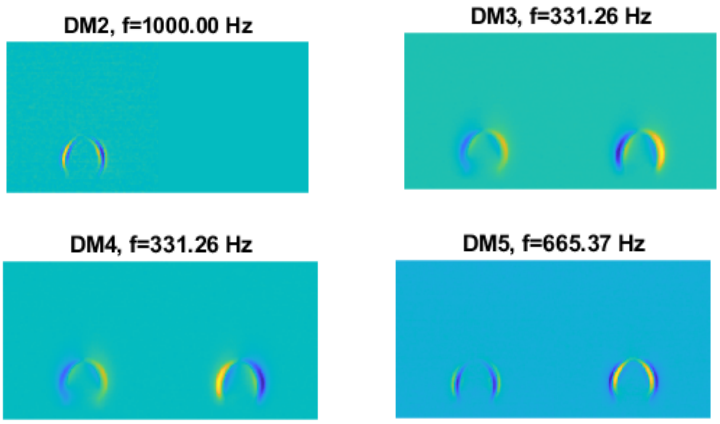

Figure 5. DMD modes with their frequencies, starting with the second mode on top on the left and ending with the fifth mode below on the right, which the real part and imaginary part of each mode being the left and right side, respectively

As mentioned in the dynamic modal decomposition (DMD) section, DMD modes are separated into real part and imaginary part. In the figures above, the left side represents the real part, while the right side represents the imaginary part of the mode. The modes represent the spatial contribution to the flow field and are supposed to display local and global features, like symmetry, mixing, transient response, and long-time behavior. For the investigation with DMD, traditionally, the modes are considered individually.

For the reason they are analyzed individually, it is possible to compare the DMD modes obtained with the POD modes. To do this, the **P**ower **S**pectral **D**ensity (PSD) of each mode is done, which is illustrated below

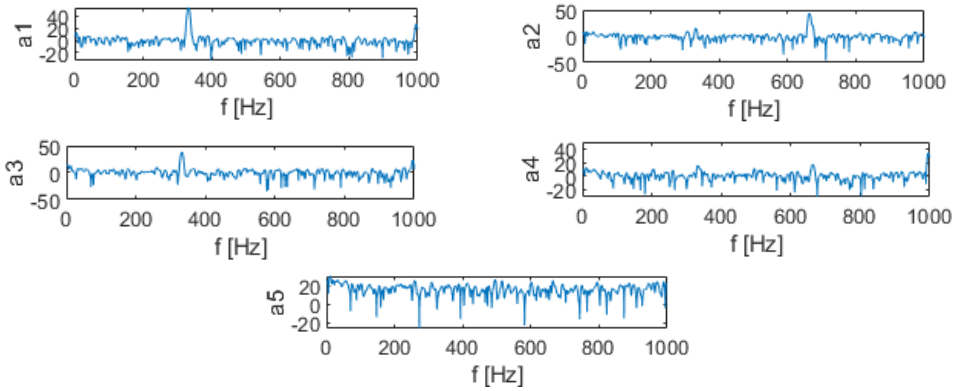

Figure 6. PSD result, relating each POD mode to the predominant frequency. For the first $\boldsymbol{a1}$ and third $\boldsymbol{a3}$ modes, the predominant frequency is approximately 330 Hz, and for the second mode $\boldsymbol{a2}$ the predominant frequency is approximately 660 Hz

By analyzing the power spectral density (PSD) result, it can be said that mode 1 and mode 3 of the POD are modes 3 and 4 of the DMD, with frequencies of 331.26 Hz respectively. While mode 2 of the POD is mode 5 of the DMD with frequency of 665.37 Hz. As already expected from the analysis made of the POD, the fourth and fifth mode have a lot of noise in their measurements, preventing an efficient result in the PSD. Observing more carefully the fourth mode of the POD, it is possible to suggest that it is the second mode of the DMD, since it seems to have a predominant frequency very close to 1000 Hz.

5. CONCLUSIONS

The above discussion is intended to elucidate the importance of image processing in eliminating as much noise as possible and, consequently, generate more accurate results for different modal decomposition's.

Furthermore, depending on the type of the problem to be analyzed, more than one type of modal decomposition can be applied, since the results obtained can be related, even if individually.

In the case of this paper, proper orthogonal decomposition (POD) and dynamic mode decomposition (DMD) were applied to the oscillatory methane jet diffusion flames data and, therefore, it was possible to perform a modal analysis of the problem, initiating the study of the jet behavior, so that in future studies, it will be possible to perform a more accurate analysis and determine the complete behavior of the flow.

6. ACKNOWLEDGEMENTS

The authors would like to thank the MAE Department at UCLA, essentially Professor Ann R. Karagozian and Andres Vargas, for the collaboration in obtaining the experimental data for this work.

7. REFERENCES

L.I. Rudin, S. Osher, E. Fatemi, 1992. *Nonlinear total variation based noise removal algorithms*. Physica D, vol.60, pp. 259-268, doi: 10.1016/0167-2789(92)90242-F

Brunton, S.L. and Kutz, J.N., 2018. *Data-Driven Science and Engineering: Machine Learning, Dynamical Systems, and Control*. Cambridge University Press.

Hyung Sub Sim, Andres Vargas, Dongchan Daniel Ahn Ann R. Karagozian, 2020. *Laminar Microjet Diffusion Flame Response to Transverse Acoustic Excitation*, Combustion Science and Technology, doi: 10.1080/00102202.2020.1726897.

Kutz, J. N., 2013. *Data-Driven Modeling Scientific Computation: Methods for Complex Systems Big Data*, Oxford Univ. Press, New York.

Kutz, J. N., Brunton, S. L., Brunton, B. W., and Proctor, J. L., 2016. *Dynamic Mode Decomposition: Data-Driven Modeling of Complex Systems*, SIAM, Philadelphia, PA.

Berkooz, G., P. Holmes, and J. L. Lumley. 1993. *The proper orthogonal decomposition in the analysis of turbulent flows*. Annu. Rev. Fluid Mech. 25 (1):539–75. doi:10.1146/annurev. fl.25.010193.002543.

Schmid, P. J. 2010. *Dynamic mode decomposition of numerical and experimental data*. J. Fluid Mech. 656:5–28. doi:10.1017/S0022112010001217.

Cordier, L., and Bergmann, M. 2008. *Proper Orthogonal Decomposition: An Overview*, Lecture Series 2002-04, 2003-03 and 2008-01 on Post-Processing of Experimental and Numerical Data, Von Karman Institute for Fluid Dynamics, VKI, 2008, p. 46.

Noack, B. R., Morzynski, M., and Tadmor, G. (eds.), 2011. *Reduced-Order Modelling for Flow Control*, Springer, New York.

Nair, A. G., Taira, K., and Brunton, S. L., 2017. *Oscillator Network Based Control of Unsteady Fluid Flows*, 20th IFAC World Congress, Paper 4192, Toulouse.

George, W. K., 1988. *Insight into the Dynamics of Coherent Structures from a Proper Orthogonal Decomposition*, Near Wall Turbulence, edited by S. Kline, and N. Afghan, Hemisphere, New York.

LeGresley, P. A., 2005. *Application of Proper Orthogonal Decomposition (POD) to Design Decomposition Methods*, Ph.D. Thesis, Stanford University, Stanford, CA.

Towne, A., Schmidt, O. T., and Colonius, T., 2018. *Spectral Proper Orthogonal Decomposition and Its Relationship to Dynamic Mode Decomposition and Resolvent Analysis*, Journal of Fluid Mechanics.

Kajishima, T., and Taira, K., 2017. *Computational Fluid Dynamics: Incompressible Turbulent Flows*, Springer, New York.

Tu, J. H., Rowley, C. W., Luchtenburg, D. M., Brunton, S. L., and Kutz, J. N., 2014. *On Dynamic Mode Decomposition: Theory and Applications*, Journal of Computational Dynamics, Vol. 1, No. 2, pp. 391–421. doi:10.3934/jcd

8. RESPONSIBILITY NOTICE

The authors are solely responsible for the printed material included in this paper.